APPLIED AND ENVIRONMENTAL MICROBIOLOGY, Feb. 1995, p. 708–717 Vol. 61, No. 2
0099-2240/95/$04.00+0

Cell Cycle Regulation in Marine *Synechococcus* sp. Strains

BRIAN J. BINDER* AND SALLIE W. CHISHOLM

Ralph M. Parsons Laboratory, Massachusetts Institute of Technology, Cambridge, Massachusetts 02139

Received 16 September 1994/Accepted 28 November 1994

The cell cycle behavior of four marine strains of the unicellular cyanobacterium *Synechococcus* sp. was analyzed by examining the DNA frequency distributions of exponentially growing and dark-blocked populations and by considering the patterns of change in these distributions during growth under a diel light-dark cycle. The two modes of cell cycle regulation previously identified in a freshwater and coastal marine *Synechococcus* isolate, respectively, were represented among the three open-ocean strains we examined. The first of these modes of regulation is consistent with the slow-growth case of the widely accepted prokaryotic cell cycle paradigm. The second appears to involve asynchronous initiation of chromosome replication, the presence of multiple chromosome copies at low growth rates, and variability in chromosome copy number among cells in the population. These characteristics suggest the involvement of a large probabilistic component in cell cycle regulation which could make the application of cell cycle-based estimators of in situ growth rate to *Synechococcus* populations problematic.

Two distinct processes are involved in the growth of any phytoplankton or microbial population: cell growth (i.e., the production of biomass) and cell division (i.e., the production of new cells). Although these two processes are usually closely coupled, each may be regulated differently by different environmental factors. For example, in many eukaryotic algae, growth (photosynthesis) and division are restricted to different times of the day (26). Because neither cell growth nor cell division can proceed for very long in the absence of the other, population growth is obviously dependent on both of these processes. Therefore, a full understanding of the dynamics of phytoplankton or microbial populations requires an understanding of cell cycle regulation in these organisms. Likewise, efforts to use cell cycle descriptors (e.g., frequency of dividing cells [16, 23] or DNA frequency distributions [6, 37]) to make inferences about the growth rate of microorganisms in situ must obviously rely on our knowledge of the cell cycle behavior of these organisms.

Prokaryotic picoplankton are responsible for a significant portion of the overall primary productivity in oligotrophic marine and freshwater ecosystems (34, 41). This group comprises the unicellular cyanobacterium *Synechococcus* spp. and the more recently described and closely related *Prochlorococcus* spp. (9, 36, 40). Our current understanding of the cell cycle in these organisms is based largely on the general prokaryotic paradigm developed originally by Cooper and Helmstetter (10) using data from studies with *Escherichia coli* and related species. However, there is evidence that some aspects of the cell cycle in a freshwater *Synechococcus* strain differ from this classical model (see below). In the present study, we examine the extent to which these differences extend to marine *Synechococcus* species.

The prokaryotic cell cycle model of Cooper and Helmstetter (10) has been reviewed extensively by many authors (11, 17, 44). For the present purposes, it is convenient to consider two general cases of the model: fast growth and slow growth. The fast-growth case applies when the generation time (T_g) is less than the sum of the time required for chromosome replication (C) and the time between the termination of replication and cell division (D). Under such conditions, C and D remain constant as growth rate (or generation time) varies. (In *E. coli* growing at 37°C, C and D are approximately 40 and 20 min, respectively [17].) Generation times shorter than $C+D$ are accomplished by the overlapping of rounds of replication. Thus, initiation of replication can occur prior to a pending division event (or, at the fastest rates, prior to the termination of the old round of replication) such that daughter cells inherit chromosomes that are already in the process of replication. In this fast-growth situation, more than one chromosome origin (each corresponding to a different whole or partially replicated chromosome) is present in a cell at the time of the initiation of replication, and such initiation occurs simultaneously at all of these origins (24). This "synchronous initiation" leads to the prediction that at any time cells may contain complete copies of the genome (and copies of the chromosome origin) only in numbers corresponding to 2^n, where n is an integer. Thus, 1, 2, 4, or 8 complete copies or origins are possible (depending on the state of the population and the values of the cell cycle parameters), but 3, 5, 6, or 7 copies are not.

In the slow-growth case of the model, when $T_g > (C+D)$, C and D may vary with growth rate, there is no overlap between rounds of replication, and each daughter cell inherits exactly one chromosome (17). This leads to another prediction of the model: that only those cells growing with $T_g < (C+D)$ will ever contain more than 2 genome equivalents of DNA.

The prokaryotic cell cycle model can be used to predict DNA frequency distributions for populations growing under specific circumstances. For example, when cells are in balanced growth their population age distribution assumes a known form, and this can be combined with the model's predicted relationship between cell age and DNA content to calculate an expected DNA frequency distribution (1, 31). For the fast-growth case, the predicted DNA frequency distributions can take on a variety of shapes, depending on the values of the parameters T_g, C, and D, but at any given growth rate [as long as $T_g < (C+D)$] the lowest DNA per cell is >1 genome equivalent (because cells inherit partially replicated chromosomes) and the highest is twice that value (excluding the Gaussian "tails" that measurement error adds to the distributions). In the case of slow growth, on the other hand, the expected

* Corresponding author. Present address: Department of Marine Sciences, Ecology Building, University of Georgia, Athens, GA 30602-2206. Phone: (706) 542-6408. Fax: (706) 542-5888. Electronic mail address: bbinder@uga.cc.uga.edu.

distributions are bimodal, with peaks corresponding to 1 and 2 genome equivalents. In this case, the DNA distribution is analogous to that obtained for eukaryotic populations, in which the first peak corresponds to cells in G1 (prior to the start of chromosome replication), the second peak corresponds to cells in G2 (those having finished DNA replication but not yet divided), and the intermediate part of the distribution corresponds to cells in S (those in the midst of DNA replication).

The synchrony of initiation at multiple origins within a given cell has been tested by examining the DNA frequency distributions of *E. coli* populations treated with rifampin or chloramphenicol (30). Under these conditions, initiation of new rounds of chromosome replication is inhibited, but extant rounds are allowed to go to completion. After such chromosome "run-out," the number of complete chromosome copies in any given cell corresponds to the number of origins present in that cell at the time of treatment. As discussed above, synchronous initiation would imply that only 2^n origins can be present in a cell at any time. Therefore, the DNA frequency distribution of a population after chromosome run-out should be composed wholly of cells with 1, 2, 4, or 8 chromosome equivalents. Skarstad et al. (30) demonstrated that this is in fact the case for wild-type *E. coli*, confirming that initiation is synchronous in these cells. However, these authors also showed that in certain replication mutants, the DNA frequency distributions included cells with a wide range of chromosome equivalents, including numbers other than 2^n (30, 32). These authors referred to the presence of such anomalous chromosome numbers as the "asynchrony phenotype," reflecting the idea that these distributions likely result from a lack of synchrony in the initiation of chromosome replication within each cell.

The extent to which the classical prokaryotic model describes the cell cycle of cyanobacteria is not well known at present. To date, the cell cycle characteristics of only two *Synechococcus* strains have been examined in detail. The results from a study involving the coastal isolate WH8101 were consistent with the slow-growth case of the model: all distributions were bimodal, with peaks corresponding to 1 and 2 genome equivalents (1). In contrast, data from a subsequent study of the freshwater strain PCC 6301 (formerly *Anacystis nidulans*) (2), along with earlier studies with this strain (22, 27, 42), were not completely compatible with the model. In particular, PCC 6301 was found to contain multiple chromosome copies even at extremely low growth rates and to contain such copies in numbers other than 2^n per cell (2). In this respect, PCC 6301 conforms to the asynchrony phenotype observed in *E. coli* replication mutants (30, 32).

To date, then, two different "modes" of cell cycle regulation have been identified within the *Synechococcus*: one operating in a coastal marine isolate, and the other operating in a freshwater isolate. The primary goal of the present study was to determine which of these modes of regulation (if either) operates in marine *Synechococcus* strains more representative of open-ocean environments. We will show that, in fact, both modes are represented in different strains within this relatively restricted taxonomic cluster. Furthermore, we will examine the consequences of these two modes of regulation on the diel cell cycle dynamics in two representative strains growing under a light-dark (LD) cycle.

MATERIALS AND METHODS

Synechococcus strains were provided by J. Waterbury (Woods Hole Oceanographic Institution, Woods Hole, Mass.) and assumed to be clonal. For comparative purposes, we chose to study the freshwater and coastal marine isolates (PCC 6301 and WH8101, respectively) which have received attention previously (see above), as well as three isolates from the open ocean (WH7803, WH7805, and WH8103). The marine strains were grown in SN medium made with GF/F-filtered Vineyard Sound seawater (40), and the freshwater strain was grown in C medium (21) buffered with 10 mM HEPES (*N*-2-hydroxyethylpiperazine-*N*′-2-ethanesulfonic acid) at pH 7.8. Culture growth was routinely monitored by in vivo fluorescence (3).

For the constant-light studies, 25-ml cultures were grown in borosilicate tubes (25 by 150 mm) at 23°C under a light intensity of approximately 30 microeinsteins $m^{-2}\ s^{-1}$ (photosynthetically active radiation, cool white fluorescent illumination, measured with a scalar irradiance meter). Cultures were periodically diluted into new medium prior to any decrease in the exponential growth rate; in this way, each culture was maintained at a constant growth rate for at least 10 generations prior to sampling.

In preparation for sampling, four replicate cultures of a particular strain were inoculated from a single tube and maintained as above for 2 days. Two of these cultures were then harvested, and the other two were put in the dark and incubated for the equivalent of three generations prior to sampling. Such a "dark-block" treatment has been hypothesized to result in chromosome run-out (see above) in *Synechococcus* populations (2). Cells were harvested and preserved in methanol as described previously (2).

For the diel cycle studies, cultures were maintained as above, at 24°C and approximately 90 microeinsteins $m^{-2}\ s^{-1}$, under a daily 14:10-h LD cycle. To allow repeated sampling over time, after 10 generations of growth in tubes, cells were inoculated into 500 ml of medium in 1-liter stirred flasks and incubated under unchanged conditions. After 4 days of growth, cells from these flasks were inoculated into fresh flasks, and the diel time courses commenced 1 day later. Over the next 72 h, 12.5 ml was sampled from each flask every 2 h. After in vivo fluorescence was measured on this sample, 9.5 ml was preserved as above for flow cytometric DNA analysis, and 1 ml was preserved with formalin (5% final concentration) and stored at 4°C for subsequent microscopic cell counts. Cell concentration and frequency of dividing cells (FDC) were determined by epifluorescence microscopy (40).

For flow cytometric analysis, aliquots of the methanol-fixed samples were washed once in phosphate-buffered saline (pH 7.5) and stained with the DNA-specific fluorochrome Hoechst 33342 (final concentration, 0.05 $\mu g\ ml^{-1}$). A standard sample, derived from a stationary-phase culture of PCC 6301 preserved as above, was included with each batch of stained samples (2). This standard was run before and after each sample as a staining control and to ensure that the instrument resolution remained maximal.

Stained samples were analyzed on a Coulter EPICS-753 flow cytometer, using 300 mW of UV laser excitation, a 33-mm-focal length spherical quartz focusing lens, and a 76-μm jet-in-air flow cell. Hoechst fluorescence was measured between 418 and 530 nm; phycobiliprotein fluorescence, used to unambiguously identify *Synechococcus* cells, was measured above 630 nm. At least 10^4 cells were analyzed for each sample. Samples from the diel experiment were analyzed in random order.

ModFit software (Verity Software House, Topsham, Maine) was used to deconvolute DNA frequency distributions. For bimodal distributions, a simple model that included two Gaussian populations (g_1 and g_2) and a broadened rectangle (s_1) was used. For multimodal distributions, the model included as many as five Gaussian populations (g_1 to g_5), with broadened rectangles between each (s_1 to s_4). In both cases, the boundaries and standard deviations (SDs) of each rectangle were set equal to the mode and SD of the adjacent gaussians. (The SDs of each compartment are assumed to reflect both measurement error and variability in staining.) These two models appeared to fit the distributions satisfactorily (Fig. 1). In a few cases, an additional gaussian was added to account for a shoulder on the g_1 peak (see Results), in which case the reported g_1 fraction included the contribution of that additional population.

For the purpose of discussion, we refer to cells with 1 genome equivalent as g_1 cells and those with 2 genome equivalents as g_2, etc.; we refer to cells with between 1 and 2 genome equivalents (which are presumably in the midst of synthesizing DNA) as s_1 and those with between 2 and 3 genome equivalents as s_2, etc. Although this terminology is obviously borrowed from the eukaryotic G1, S, and G2 cell cycle phases, in the present case we do not intend it to refer to cell cycle phases per se, but rather we use it as a simple way of referring to subpopulations of cells with different DNA contents.

The magnitudes of the cell cycle parameters *C*, *D*, and *B* were estimated from the cell cycle fractions making up bimodal DNA histograms from exponentially growing (constant light) populations, using the equations of Slater et al. (33) and assuming that the durations of the eukaryotic phases G1, S, and G2 are mathematically analogous to the prokaryotic cell cycle parameters *B*, *C*, and *D*, respectively. *C* and *D* were discussed above; *B* is the time between cell birth and the initiation of DNA replication in slowly growing cells and is often considered the simple mathematical consequence of $T_g > (C+D)$ (17).

For populations growing under a diel LD cycle, the equation of McDuff and Chisholm (23) as generalized by Carpenter and Chang (6) was used to estimate cell cycle parameters:

$$\mu = 1/(nT_x)\sum_{i=1}^{n} \ln (1 + fx_i) \quad (1)$$

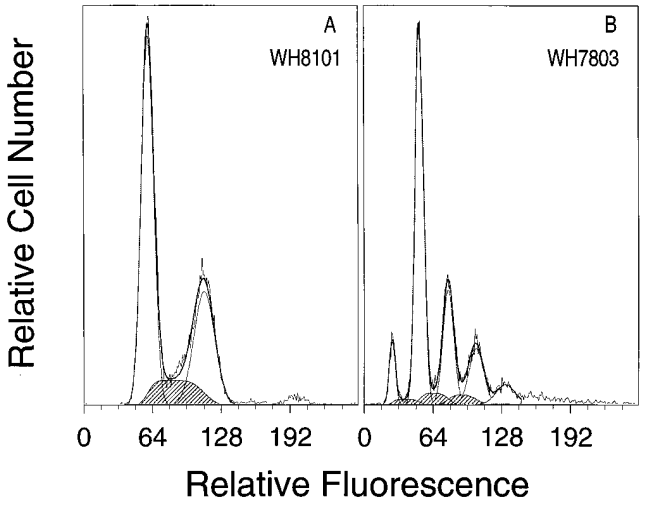

FIG. 1. Representative DNA frequency distributions and their component populations, as deconvoluted with a model made up of Gaussian populations (stippled) separated by broadened rectangles (hatched). Narrow lines show raw data; heavy lines show model fit (i.e., the sum of the fitted components). (A) WH8101; (B) WH7803.

where μ is the mean specific growth rate, T_x is the duration of terminal cell cycle event x, n is the number of sampling time points, and fx_i is the fraction of the population in terminal event x at sampling point i. The terminal event can be any cell cycle phase (or combination of phases) that ends in cell division. For a population of known μ, therefore, the values of D and $(C+D)$ can be calculated. The calculation of C and B from these values is trivial.

In order to better discern patterns in cell numbers, FDC, and DNA subpopulations over the course of the 72-h diel experiment, 6-h running averages of each of these parameters were calculated and are presented in all relevant figures. Such a running average would tend to decrease the amplitude of any periodic signal but by filtering out some of the analytical "noise," makes such signals easier to discern. As an alternate approach to this problem, we used a modified periodic function to fit the diel data (7). The function was of the form:

$$f(t) = (1 + c_0 t)\,[a_1\cos(\phi) + b_1\sin(\phi) + a_2\cos(2\phi) + b_2\sin(2\phi)]$$

where $f(t)$ is the fractional contribution of a subpopulation, t is time in hours, and $\phi = \pi t/12$. The values of a_1, a_2, b_1, b_2, and c_0 were obtained by fitting the periodic function to the data for all 3 days of the experiment, using a nonlinear least-squares curve fitter (Jandel Scientific, San Rafael, Calif.). The c_0 term was included as a simple way to accommodate noncyclic day-to-day changes.

The genome size of each *Synechococcus* strain was estimated by comparing the Hoechst fluorescence corresponding to 1 genome equivalent with that in the PCC 6301 standard. Because the Hoechst stain binds specifically to A-T base pairs, and because this binding is a nonlinear function of percent AT, these relative fluorescence values must be corrected for differences in percent AT between each sample and the standard (15). The relative genome size was therefore calculated according to the curvilinear function of Godelle et al. (15), using the known values for percent AT in the experimental and standard strains (39) and assuming that the Hoechst stain binds to a series of five A-T pairs (15). Absolute genome sizes were then calculated on the basis of a PCC 6301 genome size of 2.12×10^9 Da (18).

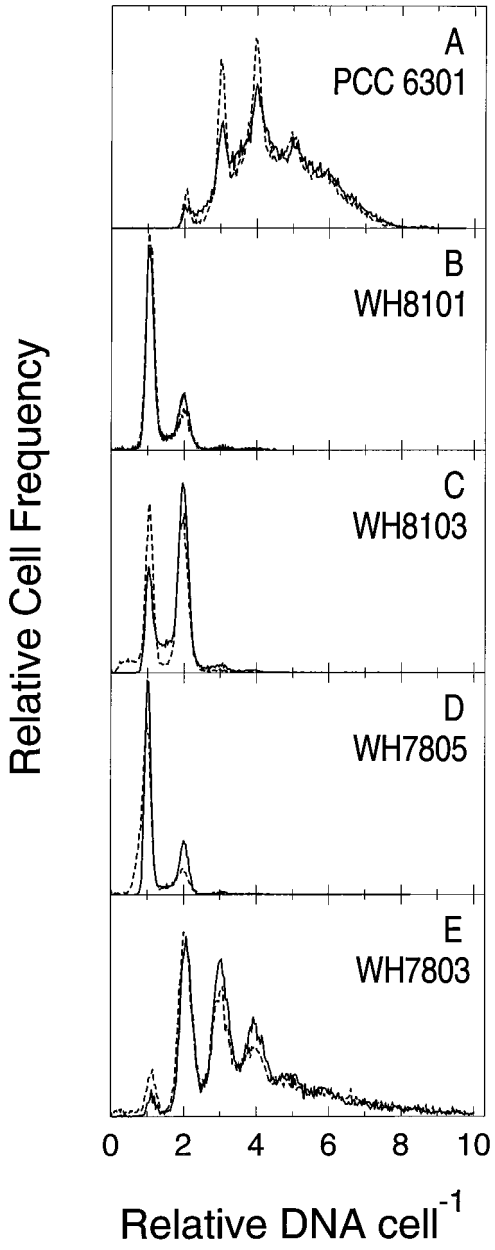

FIG. 2. DNA frequency distributions of exponentially growing, constant-light *Synechococcus* populations (solid lines) and of the same populations after the equivalent of three generations in the dark (broken lines). (A) PCC 6301; (B) WH8101; (C) WH8103; (D) WH7805; (E) WH7803.

RESULTS

Cell cycle characteristics of different *Synechococcus* strains. DNA distributions were analyzed for five strains of *Synechococcus* sp. growing at the same light intensity under constant illumination and for the same cultures after the equivalent of three generation times in the dark (Fig. 2). As expected (see above), the DNA frequency distributions for WH8101 (the coastal isolate) were bimodal, reflecting a population of cells largely containing exactly 1 or 2 genome copies (Fig. 2B). In contrast, but again as expected, DNA distributions for the freshwater strain PCC 6301 were multipeaked, and these peaks were not restricted to the set of 2^n chromosome copies as would be predicted for *E. coli*. Clear subpopulations of cells containing 2, 3, 4, and 5 genome equivalents were evident in these distributions, with a significant number of cells containing even higher amounts of DNA (Fig. 2A). Of the three remaining (open-ocean) strains, the DNA distributions for WH8103 and WH7805 were bimodal (and therefore similar to that observed in WH8101), while those for WH7803 clearly showed the asynchrony phenotype, with multiple peaks corresponding to 1, 2, 3, and 4 genome equivalents, and significant numbers of cells with higher-order copy numbers (Fig. 2E). The DNA frequency distributions for dark-blocked populations were not obviously different from the exponential distributions, although there was a decrease in the fraction of s_1 cells

TABLE 1. Cell cycle parameter estimates for *Synechococcus* strains with bimodal DNA frequency distributions[a]

Culture	Doubling time (h)	Mean ± SE (n = 2)					
		% Population[b]			Cell cycle parameter (h)[c]		
		g_1	s_1	g_2	*B*	*C*	*D*
WH8101							
Exponential							
A	16.7	67.1 ± 4.3	15.0 ± 0.5	17.9 ± 3.8	10.1 ± 0.5	3.0 ± 0.1	4.1 ± 0.9
B	17.6	63.3 ± 0.5	15.3 ± 0.2	21.4 ± 0.3	9.7 ± 0.1	3.0 ± 0.0	4.9 ± 0.1
Dark blocked							
C	16.7	71.8	12.3	15.8			
D	17.1	71.6	12.7	15.8			
WH7805							
Exponential							
A	14.9	26.8 ± 0.0	18.9 ± 0.4	54.3 ± 0.4	3.1 ± 0.0	2.5 ± 0.1	9.3 ± 0.1
B	15.3	65.7 ± 0.0	12.3 ± 0.2	22.1 ± 0.1	8.8 ± 0.0	2.1 ± 0.0	4.4 ± 0.0
Dark blocked							
C	14.7	73.6	9.3	17.1			
D	15.2	79.2	7.1	13.7			
WH8103							
Exponential							
A	23.3	28.1 ± 0.8	19.1 ± 1.0	52.7 ± 1.7	5.1 ± 0.2	4.0 ± 0.2	14.2 ± 0.4
B	21.6	17.6 ± 1.7	25.3 ± 1.8	57.1 ± 3.5	2.9 ± 0.3	4.7 ± 0.4	14.1 ± 0.7
Dark blocked							
C	22.1	38.7	9.6	51.7			
D	21.2	40.7	6.5	52.8			

[a] Four independent cultures (A to D) of each strain were analyzed; all were growing exponentially with the doubling times indicated. Cultures C and D were dark blocked prior to harvest and preservation. Standard errors refer to the analytical error of each estimate, as determined by flow cytometric analysis of two different aliquots of cultures A and B on two different days. (Replicate analyses of C and D samples were not available.)

[b] Population fractions were calculated by fitting a simple model to DNA frequency distributions as described in Materials and Methods.

[c] Cell cycle parameters were calculated with the equations of Slater et al. (33), using population fractions from the exponentially growing populations.

in dark-blocked populations with bimodal distributions (Table 1).

Estimates of the magnitude of the chromosome replication time, *C*; the postreplication time, *D*; and the prereplication period, *B*, were made for the three *Synechococcus* strains with bimodal DNA distributions (see Materials and Methods) (Table 1). The length of *C* ranged from 2.1 to 4.7 h and was significantly correlated with generation time among the three strains considered ($r = 0.91$; $P < 0.05$) (Fig. 3). On average, *C* represented approximately 17% of the total generation time. There is considerable variability in the calculated lengths of *B* and *D* among these strains and between the replicate cultures of one strain (WH7805). Values for *B* were between 3.1 and 10.1 h; those for *D* ranged from 4.1 to 14.2 h. These parameters were not correlated with generation time. Thus, although it is mathematically necessary that *B* and/or *D* increase as doubling time increases (given that the absolute increase in *C* is small), different strains appear to adjust these parameters differently. WH8103, for example, had the longest doubling time in this study, yet it had the lowest mean *B* value (4.0 h); most of its cell cycle was accounted for by *D*. In contrast, WH8101, which grew with a significantly shorter generation time, had a much higher *B* value (9.9 h).

The relative genome size of each of the *Synechococcus* strains in the present study can be estimated by comparing the magnitude of Hoechst fluorescence corresponding to a single genome equivalent in each to that in the "standard" PCC 6301 sample (see Materials and Methods) (Table 2). The calculated genome sizes (corrected for differences in percent AT) of the four marine strains analyzed here were between 1.06 and 1.41 times the PCC 6301 genome size, corresponding to between 2.2×10^9 and 3.0×10^9 Da.

Growth under an LD cycle. How are the apparent differences in cell cycle regulation in different *Synechococcus* strains reflected in populations growing under a diel LD cycle? In order to address this question, we acclimated two strains with different regulatory modes (WH8101 and WH7803) to a 14:

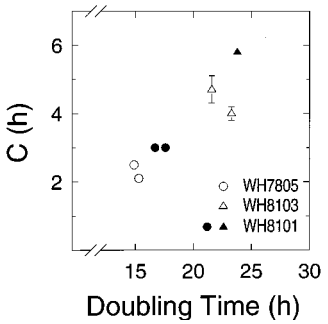

FIG. 3. Relationship between the mean chromosome replication time, *C*, and the population generation time for the three *Synechococcus* strains with bimodal DNA frequency distributions: WH8101 (●, ▲); WH7805 (○); and WH8103 (△). *C* values are from Table 1; error bars (shown when larger than symbol) reflect analytical error, as described in Table 1. The symbols ●, ○, and △ represent *C* values calculated from constant-light cultures, all growing at approximately equal light intensity and temperature as described in Materials and Methods. In contrast, the symbol ▲ represents a single value calculated for the WH8101 culture growing under a 14:10-h LD cycle, as described in the text.

TABLE 2. Estimated genome sizes of *Synechococcus* strains in this study[a]

Strain	% AT[b]	Fluorescence/genome (relative)[c]	Mean genome size	
			Relative[d]	Da (10^9)[e]
PCC 6301	45	1.01 ± 0.012	1.01	2.14
WH7803	39	0.57 ± 0.006	1.06	2.25
WH7805	40	0.69 ± 0.006	1.15	2.44
WH8101	36	0.53 ± 0.002	1.41	2.99
WH8103	41	0.72 ± 0.012	1.20	2.54

[a] Genome size comparisons were based on g_1 peak mode Hoechst fluorescence. Four independent cultures of each strain were analyzed.
[b] From reference 39.
[c] Expressed as a fraction of the mode fluorescence of the one-genome peak in the PCC 6301 standard run before and after each sample (see text). Means ± standard errors are given.
[d] Expressed as a fraction of the PCC 6301 genome, corrected for differences in percent AT according to Godelle et al. (15) (see Materials and Methods).
[e] Based on a PCC 6301 genome size of 2.12×10^9 Da (18).

10-h LD cycle and analyzed each over the course of 72 h of growth.

As expected from the results of the constant-light experiment, the DNA frequency distributions for WH8101 and WH7803 growing under a diel light cycle were dramatically different from each other (Fig. 4). (For the sake of clarity, only the day 2 distributions are presented; results for all 3 days of the experiment are summarized in Fig. 5 and 6.) In WH8101, the distributions were bimodal at all times of the day, and diel changes in the relative magnitude of different cell cycle phases were relatively subtle. In contrast, the distributions for WH7803 consistently contained multiple peaks, and the relative importance of each peak varied considerably over the course of the day. On day 2, for instance, there is a coherent trend of increasing importance of the one-genome peak at the expense of the higher-order peaks as the day progresses. This trend is evident on all 3 days of the experiment, although its magnitude varies from day to day. The fact that in WH7803 the distribution at the start of day 2 is obviously different from that

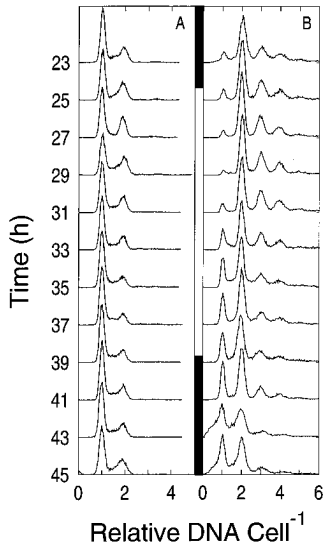

FIG. 4. DNA frequency distributions for WH8101 (A) and WH7803 (B) on day 2 of the 72-h diel LD experiment. Numbers on the *y* axis refer to the experimental sampling time. Distributions adjacent to the filled vertical bars correspond to dark time points.

at the end of the day is a reflection of the significant day-to-day variability we observed in this culture over the course of the experiment (see Fig. 6 and below).

The 43- and 45-h DNA distributions for WH7803 include a shoulder at the low end of the g_1 peak (Fig. 4B). This shoulder appears in samples from approximately the same time of day (i.e., the middle of the dark period) on days 1 and 3 as well but not in any samples of WH8101. We believe that this shoulder is the result of decreased staining efficiency in WH7803 cells at this particular time of day: the shoulder decreased markedly as staining time increased from 15 min to 4 h in these samples, while samples from other times of the day remained unaffected (data not shown). There is no evidence of this phenomenon in the other strains we examined, although these were not grown under a diel LD regimen. Diel changes in stainability have obvious implications for analyzing *Synechococcus* DNA distributions in field populations.

In both *Synechococcus* strains, increases in cell number were largely concentrated in the light period (Fig. 5A and 6A). In WH8101, cell numbers increased approximately twofold over the course of each day. Daily growth was less consistent in WH7803: cell numbers increased approximately twofold on the first and last days but threefold on the middle day. The latter observation may mean that despite our best efforts, and notwithstanding a growth pattern that is indistinguishable from exponential when only noon samples are considered (data not shown), the WH7803 culture was not in steady state over the course of the experiment (owing, for example, to some sort of perturbation at the start of the experiment). Alternatively, this sort of pattern might be characteristic of populations with the asynchrony phenotype (see Discussion).

FDC showed a marked periodicity in both strains, increasing after dawn and reaching a peak 6 to 10 and 9 to 11 h later in WH8101 and WH7803, respectively (Fig. 5B and 6B). In WH8101, maximum FDC never exceeded 11%. After peaking, FDC in this strain decreased until the onset of darkness to a minimum of 4.5 to 6% and remained approximately constant throughout the dark period. In contrast, the daily peak FDC in WH7803 ranged from 20 to 27%, and (at least over the first 2 days) FDC in this strain continued to drop throughout the dark period (to a minimum of ~7%) until the onset of light the next morning.

Diel changes in the cell cycle fractions of the WH8101 population were relatively simple and reproducible from day to day (Fig. 5C). The same general trends were revealed by the periodic function fit to the data (broken lines) as by the running averages (solid lines). The g_1 fraction reached a minimum early in the light period; increased to a maximum just before the onset of darkness; after a short decrease, appeared to remain constant through the night; and finally decreased to the morning minimum again. The s_1 fraction appeared to have two daily peaks, the first coinciding with the minimum in g_1 and the second occurring 2 h after the onset of darkness. This fraction decreased throughout the remainder of the night and then increased rapidly with the onset of light to its morning maximum. The g_2 fraction peaked in the first 2 h of the light period, decreased thereafter until the onset of darkness, and then increased into the early part of the next morning. Although relatively consistent, none of these patterns involved very dramatic changes in cell cycle proportions. The fraction of g_1 cells, for example, varied from a low of 47% to a high of 62% throughout the 72 h of the experiment.

The changes in WH7803 cell cycle fractions over the 72-h time course were more complex and less consistent from day to day (Fig. 6C and D). The periodic function fit this data much less successfully, presumably owing to the lack of daily consis-

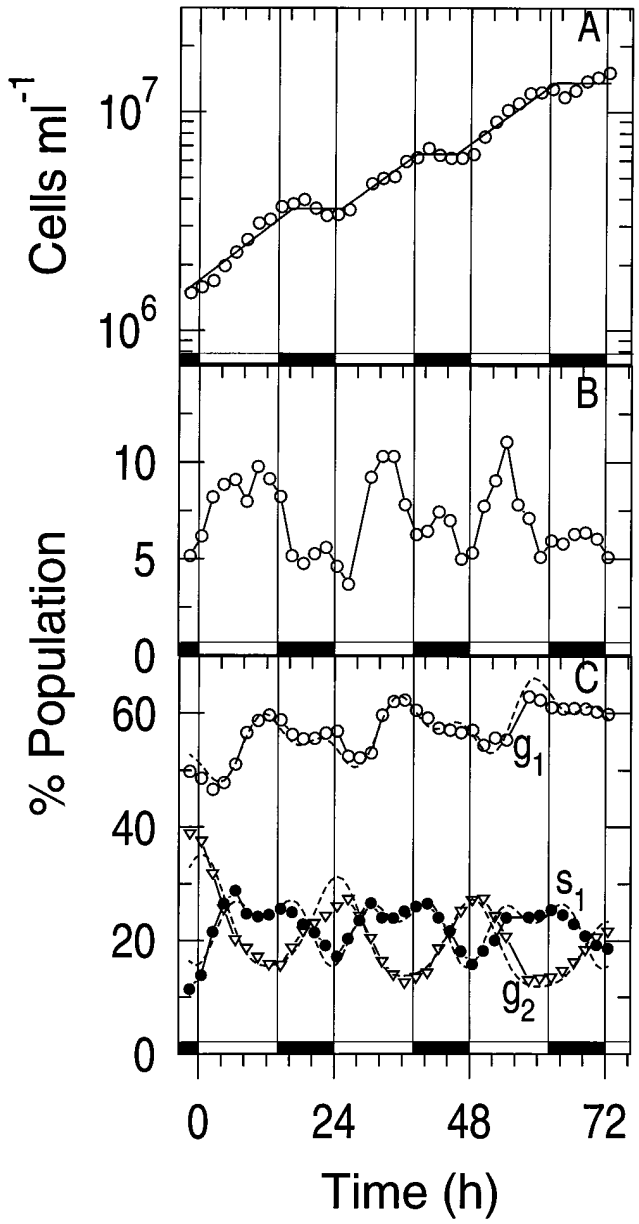

FIG. 5. Cell number (A), FDC (percentage) (B), and cell cycle fractions (C) for WH8101 growing under a 14:10-h LD cycle. Symbols are 6-h running averages of data. The solid line in panel A is the best fit of the raw data to an alternating series of exponential and stationary growth phases; the broken lines in panel C represent the periodic function fit to the raw cell cycle fraction data. Cell cycle fractions were derived from deconvolution of the DNA frequency distributions (Fig. 4), as described in the text: ○, g_1 cells; ●, s_1 cells; △, g_2 cells. Filled horizontal bars indicate dark period.

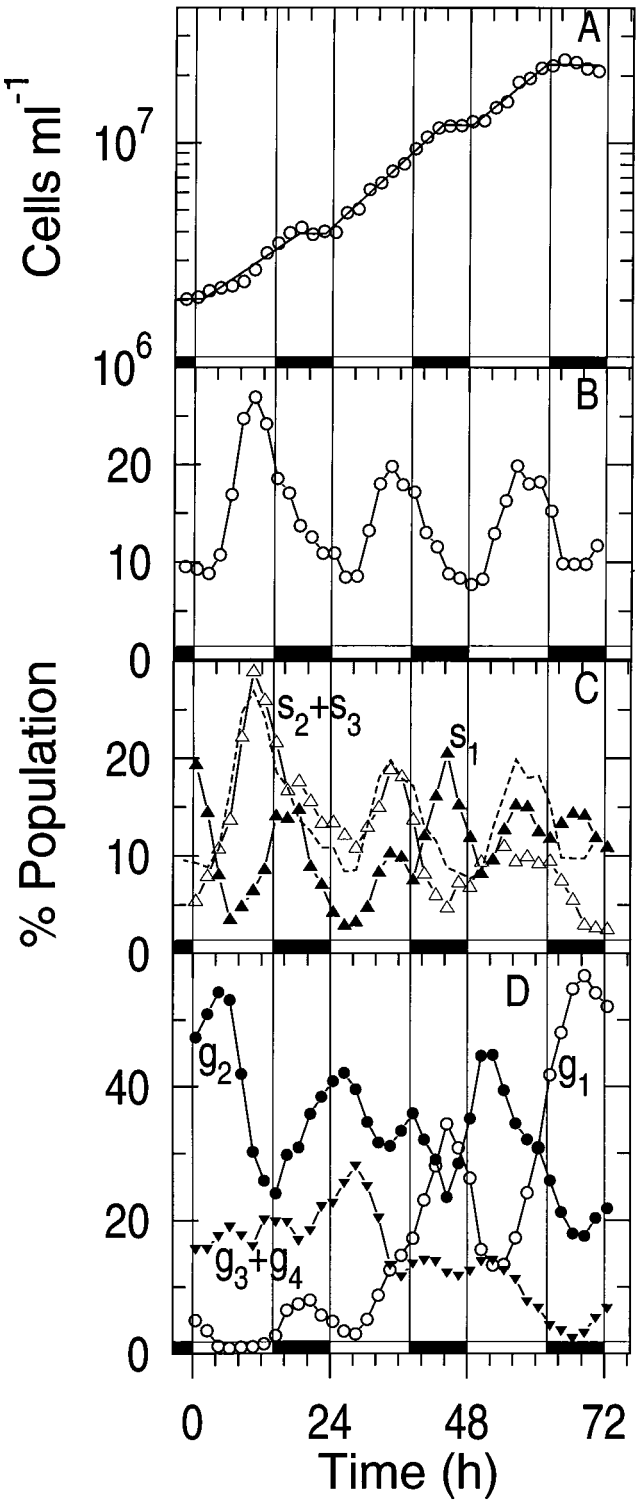

FIG. 6. Cell number (A), FDC (B), and cell cycle fractions (C and D) for WH7803 growing under a 14:10-h LD cycle. Symbols and lines in panels A and B are described in the legend to Fig. 5. (C) ▲, s_1 cells; △, s_2+s_3 cells. Broken line denotes FDC data from panel B, replotted for comparison. (D) ○, g_1 cells; ●, g_2 cells; ▼, g_3+g_4 cells.

tency (fit not shown). Nevertheless, some diel patterns could be discerned. Overlaying the obvious increase in the fraction of g_1 cells over the 3 days of the experiment, for instance, a daily maximum occurred in the middle of each night, with a corresponding minimum occurring during the day. The g_2 fraction showed a roughly inverse pattern, peaking during the day and reaching a minimum at night. Higher-order complete genome fractions (i.e., g_3 and g_4 cells) represented a relatively constant fraction of the population (15 to 20%) for the first 20 h of the experiment. After that time, these cells followed a pattern that roughly paralleled that for g_2 cells (with a peak during the day

and a trough at night), except that their contribution to the total population decreased over the remainder of the experiment. The maximum fraction of the population that these cells represented was 28%.

As was the case for WH8101, there appeared to be two daily peaks in the s fractions in WH7803, the first occurring approximately 4 h prior to the onset of darkness and the second occurring in the middle of the dark period (Fig. 6C). These two peaks were made up of different proportions of s_1 and higher-order s cells on each day of the experiment. On the first day, s_2 and s_3 cells were responsible for the afternoon peak and s_1 cells were responsible for the night peak; on the second day, there was an obvious secondary peak in s_1 cells that coincided with the afternoon peak of the s_2+s_3 cells; and on the third day, the majority of cells in both peaks were s_1 cells. The daily peak in FDC in this culture coincided very closely with the afternoon peak in s-phase cells. Particularly intriguing in this regard is the close quantitative correspondence between FDC and the fraction of s_2+s_3 cells over the first 2 days of the experiment (Fig. 6C).

DISCUSSION

The *Synechococcus* cell cycle. The DNA distributions presented here for the coastal *Synechococcus* isolate WH8101 and the freshwater strain PCC 6301 are consistent with previously published results for these strains (1, 2). The simple bimodal distributions in WH8101 conform to the slow-growth case of the Cooper-Helmstetter model (10), whereas the multimodal distributions in PCC 6301 are consistent with the asynchrony phenotype defined in *E. coli* replication mutants by Skarstad et al. (30, 32). We take these two patterns to reflect two different modes of cell cycle regulation in different *Synechococcus* strains: in the first, cells are born with one chromosome, begin replication of that chromosome after *B* min, complete replication *C* min later, and finally divide *D* min after that. A complete model for the alternate mode of regulation has not yet been put forward, but it involves inheritance of multiple genome copies even at relatively slow growth rates and the asynchronous initiation of replication of each of these copies. These two characteristics are not necessarily connected, although it should be noted that in the absence of multiple genome copies the factors that might otherwise result in the asynchrony phenotype (e.g., disrupted timing of initiation) would not be detectable with the approach taken in the present study.

We hypothesize that the presence of multiple genome copies and asynchronous initiation are indeed connected in *Synechococcus* spp. and that both reflect a large stochastic component in the cell cycle. In this view, the initiation of replication at any particular chromosome origin is highly probabilistic (although certainly not without deterministic constraints), and the timing of cell division is not rigidly connected to replication of any particular chromosome. This view is consistent with the observation that asynchrony-phenotype DNA frequency distributions generally encompass a greater-than-twofold range of cellular DNA, implying that cells in these populations are not always born with (and do not always divide with) the same number of chromosome copies. This means that there is no single "cell cycle" (defined here as the pattern of change in DNA content that a cell experiences between birth and division) through which all cells in the population pass.

It is important to note that although in this discussion we assume that the asynchrony phenotype reflects truly asynchronous initiation of chromosome replication, alternate explanations for this phenotype exist, including abortive initiation, selective chromosome degradation, and asymmetrical chromosome partitioning (29). Our probabilistic view of the *Synechococcus* cell cycle is consistent with any of these particular mechanisms underlying the observed DNA distributions.

None of the remaining *Synechococcus* species we examined in the present study (WH8103, WH7803, and WH7805) have been previously analyzed with respect to their cell cycle. These strains are all classified by Waterbury and Rippka (39) to be within the *Synechococcus* marine cluster A: they contain phycoerythrin as their major light-harvesting pigment and as a group are considered most representative of open-ocean *Synechococcus* species. WH7803 and WH7805 belong to a single immunochemically defined *Synechococcus* cluster (4) but fall into distinct taxonomic clusters on the basis of restriction fragment length polymorphism analysis (13, 43).

Examples of both modes of cell cycle regulation were evident among the three open-ocean strains we examined. The presence of the asynchrony phenotype in WH7803 indicates that this characteristic is not a peculiarity of PCC 6301 (until now the only *Synechococcus* species in which the phenotype had been observed) but rather may be present in many *Synechococcus* strains. Attempts to model in situ *Synechococcus* cell cycles (e.g., for the estimation of growth rates from DNA frequency distributions) must therefore take into account the possibility of either mode of cell cycle regulation.

For all of the bimodal strains examined, the fraction of s_1 cells was lower in the dark-blocked populations than in the corresponding exponential ones (Table 1). This observation is consistent with the hypothesis that in *Synechococcus* spp. dark blocking results in chromosome run-out, analogous to that observed in *E. coli* after inhibition of protein or RNA synthesis (1, 2, 30). However, the persistence of a significant number of s_1 cells even after the equivalent of three generation times in the dark (particularly in WH8101) implies that such run-out is incomplete in these strains.

Our estimates of *C*, the chromosome replication time, for WH8101 (~3 h) are consistent with those made by Armbrust et al. (1) for the same strain (2.4 to 4.4 h). However, the correlation observed here between *C* and generation time among different strains contrasts with the conclusion of Armbrust et al. (1) that in a single species (WH8101) *C* remains constant as growth rate varies. These two sets of observations are not necessarily mutually exclusive: it may be that among different species, *C* is correlated with growth rate under a given set of environmental conditions (i.e., that slower growers have longer chromosome replication times), whereas within a species, *C* remains constant as growth rate varies (see discussion below about cell cycle parameters in the diel LD experiment, however).

The *C* values we measured for all of the *Synechococcus* strains with bimodal distributions (2.1 to 4.7 h) are of the same order as that in *E. coli* growing at 21°C (2.2 h), despite the fact that *E. coli* generation times at that temperature are at least an order of magnitude less than the *Synechococcus* generation times (25). Given the comparable chromosome sizes of *Synechococcus* spp. and *E. coli* (see below), it appears that the slow growth rates of *Synechococcus* spp. generally (compared with *E. coli*) are not reflected in proportionately slow DNA chain elongation rates. This observation is consistent with the assertion that the molecular machinery of replication in cyanobacteria is not fundamentally different from that in *E. coli* (12).

Our estimates of *B* and *D* varied widely among the three *Synechococcus* strains with bimodal distributions, although the values for WH8101 were again consistent with those reported previously (1). The reason for the dramatic difference between the estimated lengths of *D* (and, necessarily, of *B*) in two

replicate cultures of WH7805 remains unknown at present. Neither culture showed any anomaly in terms of growth or flow cytometric signature, and the differences between the two replicates were confirmed by flow cytometric analysis of the same samples on different days (Table 1). It is interesting to note that in *E. coli* the variability in *B* and *D* both among and within slowly growing strains has also been found to be quite large (17).

The estimated genome size of the marine *Synechococcus* strains in the present study varied from 2.2×10^9 to 3.0×10^9 Da (Table 1). These values fall within the range of those tabulated by Herdman et al. (18) for a wide range of *Synechococcus* species.

Growth under a diel LD cycle. The patterns of cell growth and cell cycle phase changes observed here in WH8101 growing on a diel LD cycle are consistent with earlier observations of this strain (1). In general, the decrease in s_1 cells during the dark period, the concomitant increase in g_2 cells, and the decrease in dividing cells are consistent with the presence of dark-block points both before and after chromosome replication. Thus, darkness appears to inhibit new initiations of replication, while ongoing rounds continue. However, as noted above for dark-blocked cultures, replication does not appear to go to completion in all cells; this may reflect a lengthening of *C* under dark conditions. The persistence of dividing cells (as defined morphologically) through the night, albeit at low frequency, has been observed previously in this and other *Synechococcus* species (1, 5, 14, 40) and again (in the apparent absence of increases in cell number) is consistent with the presence of a block point after replication (during the time that cells are visibly dividing).

It is possible that the two peaks observed in the s_1 cell fraction over the course of the day reflect two cohorts of cells, the first having been blocked by the onset of darkness prior to replication and the second having been blocked after replication but before division. The presence of only one peak in both g_1 and g_2 cells does not exclude this possibility: the absence of an afternoon peak in g_2 following the first s_1 peak, for instance, could have resulted from the concomitant loss of g_2 cells (in the second cohort) through division and formation of new g_1 cells (Fig. 5C).

Note that although we refer here and elsewhere to the effect of darkness on the cell cycle, in the case of the diel experiment we cannot distinguish between a direct effect of darkness and an effect mediated by an endogenous clock. Recent studies have presented strong evidence that circadian rhythms do operate in *Synechococcus* species (19, 20, 35). The block points we infer to exist in the LD experiments could well be influenced by such rhythms and therefore may not be the direct result of darkness. Thus, the observed patterns might persist in constant light once the population has been entrained on an LD cycle. This possibility awaits further experimental investigation.

In WH7803, the diel changes in FDC observed here were consistent with most previous observations on this strain (5, 40), although in one study involving very slow growth under a 12:12-h LD regime, the FDC peak was displaced into the dark period (35). As was the case for WH8101, FDC remained significantly above zero throughout the diel cycle. In contrast to WH8101, however, WH7803 FDC appeared to decrease throughout the dark period (at least on days 1 and 2) rather than remain constant. Similar decreases in FDC during the night were observed by Campbell and Carpenter (5) and Waterbury et al. (40) for the same strain growing at a comparable growth rate. Since we presume that the only way to lose dividing cells is through cell division, a decrease in FDC necessitates an increase in cell number. In the present study, the observed change in FDC over the dark period would result in a 10% increase in cell number, an increase that could easily be accommodated by the cell count data (Fig. 6A). Thus, it appears that the dark inhibition of cell division in this strain is weaker than in WH8101.

The pattern of variation in cell cycle fractions in WH7803 during the diel experiment is complex and difficult to interpret unambiguously. This could be a reflection of both the presence of multiple block points (as discussed above) and a large stochastic cell cycle component (which would tend to distort any cell cycle phasing and could lead to variation in the amount of DNA that cells inherit and pass on). The pattern is undoubtedly complicated further by the possibly non-steady-state nature of WH7803 growth during the experiment and the fact that on day 2 the population more than doubled.

Despite these problems, some consistent diel patterns are evident. First, there is a nightly maximum in the g_1 fraction. This is in contrast to WH8101, in which g_1 declined slightly or remained constant during the night. This difference could be related to the hypothesized continuation of some cell division in the night in WH7803 but not in WH8101.

As hypothesized above for WH8101, the two daily peaks we observed in the s fractions in WH7803 may reflect the presence of two different cohorts of cells (blocked by darkness at different points in the cell cycle). The significance of the fact that the earlier s peak was composed largely of s_2 and s_3 cells and the later one was made up of s_1 cells (during the first two days) remains unknown at present. The close numerical correspondence of s_2+s_3 with the FDC (both of which were determined on different aliquots by different techniques and are computationally independent of each other) during the first two days of the experiment suggests that it is the s_2 and s_3 cells themselves that are dividing (Fig. 6C). This is a surprising result; there is no a priori reason to expect that these cells (instead of g_2 and g_3 cells, for instance) would be actively dividing. However, such a situation is by no means impossible: division by cells which are actively replicating DNA is an integral part of the fast-growth case of the classical prokaryotic cell cycle model (10). In the present case, division of an s_2 cell could result in the production of a g_1 and an s_1 cell or two s_1 cells. In fact, the lack of significant numbers of g_1 cells between hours 6 and 14 on the first day, when s_1 cells were increasing rapidly, implies that either g_1 cells have an extremely short lifetime or (more likely) there is another source for s_1 cells. This source could be division by s_2+s_3 cells, which were numerous during the same time period.

If our view of the WH7803 cell cycle is correct, cells grouped within a given compartment, as defined by DNA content, may in fact be in different cell cycle phases (with respect to cell division). For example, g_2 cells may be ready to divide (having just completed replication of a single chromosome), or they may be the product of a recent division (of a cell with higher-order copy numbers). Thus, we hypothesize that the large drop in g_2 cells between hours 6 and 12 on day 1 (in the absence of an increase in g_1 cells) reflects DNA synthesis in these cells to form g_3 or g_4 cells (which did in fact increase until hour 12). In contrast, the large decrease in g_2 cells on day 3 appeared to result from division and the formation of g_1 cells, which increased dramatically.

Implications for cell cycle-based estimates of in situ growth rate. There has been much interest in recent years in using cell cycle parameters (i.e., FDC or DNA frequency distributions) to estimate in situ growth rates of natural phytoplankton populations in general (6, 8, 23, 38) and of *Synechococcus* populations in particular (reviewed in reference 41). Such estimates

are presumed to be independent of grazing and other losses (although see reference 28) and, being based on instantaneous measurements of the natural population, are free of bottle incubation artifacts. These cell cycle approaches generally are based on equation 1 (see Materials and Methods), which relates the growth rate of a population of cells, μ, to the average fraction of the population (over the course of a 24-h period) observed to be in a "terminal" cell cycle event (i.e., a cell cycle phase that ends in cell division) and the length of that terminal event, T_x. For studies using FDC, the terminal event is defined as the portion of the cell cycle during which cells are observably dividing; for those studies using cell cycle fractions derived from DNA frequency distributions, it can be defined (for eukaryotes) as G2 + mitosis or S + G2 + mitosis (6). An important assumption that underlies equation 1 is that T_x is constant. The presence of a dark-block point within the terminal event would be expected to have the effect of lengthening that event for the subpopulation of cells that are blocked there by the onset of darkness. Therefore, the calculated μ for the overall population would overestimate the true μ, and in the same way the calculated T_x for a population growing at a known rate would overestimate the true (nonblocked) T_x. These problems would not occur if dark-block points were confined to nonterminal cell cycle events (e.g., G1, as in the model of Carpenter and Chang [6]).

Notwithstanding the presence of block points after replication (and therefore within the terminal event) and their potential artifacts, equation 1 yielded estimates of cell cycle phases in WH8101 growing on an LD cycle that are consistent with estimates from constant-light cultures that are free of such artifacts. Because the constant-light WH8101 culture in the present study was growing considerably faster than the LD culture, direct comparisons are difficult. But the values for B and D estimated from the diel culture here (11.5 and 6.4 h) are very close to those estimated by Armbrust et al. (1) for constant-light cultures of the same strain growing at a comparable growth rate (10.9 and 7.3 h, respectively). Furthermore, the calculated value of C for the LD culture (5.8 h), though considerably higher than that for the faster-growing constant-light culture in the present study, appears to conform to the relationship between generation time and C that we observed among the three *Synechococcus* species for which the calculations could be made (Fig. 3). This observation contrasts, however, the assertion by Armbrust et al. (1) that C does not vary with growth rate in WH8101, although the very low growth rates that supported that assertion in that paper have not been duplicated here. In general, the presence of dark-block points after chromosome replication in WH8101 does not appear to significantly affect the estimates of the length of cell cycle phases.

Although this conclusion alone would imply that cell cycle approaches for estimating in situ growth rate should be applicable to *Synechococcus* populations (at least those with bimodal DNA frequency distributions), the observed change in the magnitudes of C and D with growth rate makes the assumption of a single value for T_x ($= D$ or $C+D$) impossible. Carpenter and Chang (6) developed an elegant method for calculating the value of T_x from the data itself, but this method requires that the population be sufficiently phased so that the time difference between successive peaks in the fractions of S and G2 cells is identifiable. The patterns of s_1 and g_2 fractions we observed in WH8101 make such identification difficult (Fig. 5C). We observed two peaks in the s_1 fraction and one in the g_2 fraction. If we use the first s_1 peak, the calculated μ is extremely low; if we use the second, the estimate is 0.54 day^{-1}, or 23% less than the true growth rate. (Iteration per reference 6 failed to improve the estimate.) Given the amount of uncertainty regarding cell cycle behavior in *Synechococcus* spp. and the number of assumptions that must be made in applying the method thereto, we consider this estimate to be remarkably close to the true value. Without further data, however, we cannot be sure that this result is not completely fortuitous.

In contrast to these results for WH8101, natural marine *Prochlorococcus* populations appear to be tightly phased (38, 37). The time difference between the peaks in s_1 and g_2 is therefore easily observed, allowing the in situ growth rate of these populations to be estimated with reasonable confidence (37).

Application of the Carpenter and Chang approach to WH7803 and other *Synechococcus* populations with the asynchrony phenotype is problematic because no single terminal event is identifiable: at any given time, some cells are presumably cycling between 1 and 2 chromosomes and some are cycling between 2 and 4, etc. Thus, as discussed previously, g_2 cells could be composed of both newborn cells and cells preparing to divide. FDC, on the other hand, might in theory still be used to estimate growth rate in these populations: regardless of their DNA content, all cells must by definition go through a "dividing cell" stage prior to cell division. The duration of division (T_d) calculated for WH7803 in the diel study here was 3.4 h, well within the range of the values calculated for this and other *Synechococcus* strains growing at relatively high growth rates under a variety of conditions (5, 14). Application of the FDC approach to field populations will of course still involve the assumption of a constant and known T_x and is subject to the potential artifacts from cell cycle arrest discussed above.

ACKNOWLEDGMENTS

We gratefully acknowledge the expert and enthusiastic technical assistance of Michelle Bell. Comments on the manuscript by D. Vaulot were greatly appreciated.

This work was supported in part by the National Science Foundation (grants OCE-9000043, -9302529, and -9223793) and the Department of Energy Ocean Margins Program (grant DE-FG02-93er61694,A000).

REFERENCES

1. **Armbrust, E. V., J. D. Bowen, R. J. Olson, and S. W. Chisholm.** 1989. Effect of light on the cell cycle of a marine *Synechococcus* strain. Appl. Environ. Microbiol. **55:**425–432.
2. **Binder, B. J., and S. W. Chisholm.** 1990. Relationship between DNA cycle and growth rate in *Synechococcus* sp. strain PCC 6301. J. Bacteriol. **172:** 2313–2319.
3. **Brand, L. E., R. R. L. Guillard, and L. S. Murphy.** 1981. A method for rapid and precise determination of acclimated phytoplankton reproduction rates. J. Plankton Res. **3:**193–201.
4. **Campbell, L.** 1988. Identification of marine chroococcoid cyanobacteria by immunofluorescence, p. 208–229. *In* C. M. Yentsch, F. Mague, and P. K. Horan (ed.), Immunochemical approaches to estuarine, coastal, and oceanographic questions. Coastal and estuarine lecture series XXV. Springer, Berlin.
5. **Campbell, L., and E. J. Carpenter.** 1986. Diel patterns of cell division in marine *Synechococcus* spp. (cyanobacteria): use of the frequency of dividing cells technique to measure growth rate. Mar. Ecol. Prog. Ser. **32:**139–148.
6. **Carpenter, E. J., and J. Chang.** 1988. Species-specific phytoplankton growth rates via diel DNA synthesis cycles. I. Concept of the method. Mar. Ecol. Prog. Ser. **43:**105–111.
7. **Chang, J., and E. J. Carpenter.** 1990. Species-specific phytoplankton growth rates via diel DNA synthesis cycles. IV. Evaluation of the magnitude of error with computer-simulated cell populations. Mar. Ecol. Prog. Ser. **65:**293–304.
8. **Chang, J., and E. J. Carpenter.** 1991. Species-specific phytoplankton growth rates via diel DNA synthesis cycles. V. Application to natural populations in Long Island Sound. Mar. Ecol. Prog. Ser. **78:**115–122.
9. **Chisholm, S. W., R. J. Olson, E. R. Zettler, R. Goericke, J. B. Waterbury, and N. A. Welschmeyer.** 1988. A novel free-living prochlorophyte abundant in the oceanic euphotic zone. Nature (London) **334:**340–343.
10. **Cooper, S., and C. E. Helmstetter.** 1968. Chromosome replication and the division cycle of *Escherichia coli* B/R. J. Mol. Biol. **31:**519–540.

11. **Donachie, W. D.** 1981. The cell cycle of *Escherichia coli*. Soc. Exp. Biol. Semin. Ser. **10:**63–83.
12. **Doolittle, W. F.** 1979. The cyanobacterial genome, its expression, and the control of that expression. Adv. Microb. Physiol. **20:**1–102.
13. **Douglas, S. E., and N. Carr.** 1988. Examination of genetic relatedness of marine *Synechococcus* spp. by using restriction fragment length polymorphisms. Appl. Environ. Microbiol. **54:**3071–3078.
14. **Fahnenstiel, G. L., T. R. Patton, H. J. Carrick, and M. J. McCormick.** 1991. Diel division cycle and growth-rates of *Synechococcus* in Lakes Huron and Michigan. Int. Rev. Gesamten Hydrobiol. **76:**657–664.
15. **Godelle, B., D. Cartier, D. Marie, S. C. Brown, and S. Siljak-Yakovlev.** 1993. Heterochromatin study demonstrating the non-linearity of fluorometry useful for calculating genomic base composition. Cytometry **14:**618–626.
16. **Hagström, Å, U. Larsson, P. Horstedt, and S. Normark.** 1979. Frequency of dividing cells, a new approach to determination of bacterial growth rates in aquatic environments. Appl. Environ. Microbiol. **37:**805–812.
17. **Helmstetter, C. E.** 1987. Timing of synthetic activities in the cell cycle, p. 1594–1605. *In* F. C. Neidhardt, J. L. Ingraham, K. B. Low, B. Magasanik, M. Schaechter, and H. E. Umbarger (ed.), *Escherichia coli* and *Salmonella typhimurium*: cellular and molecular biology. American Society for Microbiology, Washington, D.C.
18. **Herdman, M., M. Janvier, R. Rippka, and R. Y. Stanier.** 1979. Genome size of cyanobacteria. J. Gen. Microbiol. **111:**73–85.
19. **Huang, T.-C., J. Tu, T.-J. Chow, and T.-H. Chen.** 1990. Circadian rhythm of the prokaryote *Synechococcus* sp. RF-1. Plant Physiol. **92:**531–533.
20. **Kondo, T., C. A. Strayer, R. D. Kulkarni, W. Taylor, M. Ishiura, S. S. Golden, and C. H. Johnson.** 1993. Circadian rhythms in prokaryotes: luciferase as a reporter of circadian gene expression in cyanobacteria. Proc. Natl. Acad. Sci. USA **90:**5672–5676.
21. **Kratz, W. A., and J. Meyers.** 1955. Nutrition and growth of several blue-green algae. Am. J. Bot. **42:**282–287.
22. **Mann, N., and N. G. Carr.** 1974. Control of macromolecular composition and cell division in the blue-green alga *Anacystis nidulans*. J. Gen. Microbiol. **83:**399–405.
23. **McDuff, R. E., and S. W. Chisholm.** 1982. The calculation of *in situ* growth rates of phytoplankton populations from fractions of cells undergoing mitosis: a clarification. Limnol. Oceanogr. **27:**783–788.
24. **Nordstrom, K.** 1993. Cell-cycle specific initiation of replication. Mol. Microbiol. **10:**457–463.
25. **Pierucci, O.** 1972. Chromosome replication and cell division in *Escherichia coli* at various temperatures of growth. J. Bacteriol. **109:**848–854.
26. **Prézelin, B. B.** 1992. Diel periodicity in phytoplankton productivity. Hydrobiology **238:**1–35.
27. **Roberts, T. M., L. C. Klotz, and A. A. Loeblich III.** 1977. Characterization of a blue-green algal genome. J. Mol. Biol. **110:**341–361.
28. **Sherr, B. F., E. B. Sherr, and J. McDaniel.** 1992. Effect of protistan grazing on the frequency of dividing cells in bacterioplankton assemblages. Appl. Environ. Microbiol. **58:**2381–2385.
29. **Skarstad, K., and E. Boye.** 1988. Perturbed chromosome replication in *recA* mutants of *Escherichia coli*. J. Bacteriol. **170:**2549–2554.
30. **Skarstad, K., E. Boye, and H. B. Steen.** 1986. Timing of initiation of chromosome replication in individual *Escherichia coli* cells. EMBO J. **5:**1711–1717.
31. **Skarstad, K., H. B. Steen, and E. Boye.** 1985. *Escherichia coli* DNA distributions measured by flow cytometry and compared with theoretical computer simulations. J. Bacteriol. **163:**661–668.
32. **Skarstad, K., K. von Meyenburg, F. G. Hansen, and E. Boye.** 1988. Coordination of chromosome replication initiation in *Escherichia coli*: effects of different *dnaA* alleles. J. Bacteriol. **170:**852–858.
33. **Slater, M. L., S. O. Sharrow, and J. C. Gart.** 1977. Cell cycle of *Saccharomyces cerevisiae* in populations growing at different rates. Proc. Natl. Acad. Sci. USA **74:**3850–3854.
34. **Stockner, J. G., and N. J. Antia.** 1986. Algal picoplankton from marine and freshwater ecosystems: a multidisciplinary perspective. Can. J. Fish. Aquat. Sci. **43:**2472–2503.
35. **Sweeney, B. M., and M. B. Borgese.** 1989. A circadian rhythm in cell division in a prokaryote, the cyanobacterium *Synechococcus* WH7803. J. Phycol. **25:**183–186.
36. **Urbach, E., D. L. Robertson, and S. W. Chisholm.** 1992. Multiple evolutionary origins of prochlorophytes within the cyanobacterial radiation. Nature (London) **355:**267–270.
37. **Vaulot, D., D. Marie, R. J. Olson, and S. W. Chisholm.** Submitted for publication.
38. **Vaulot, D., and F. Partensky.** 1992. Cell-cycle distributions of Prochlorophytes in the north-western Mediterranean Sea. Deep Sea Res. Part A Oceanogr. Res. Pap. **39:**727–742.
39. **Waterbury, J. B., and R. Rippka.** 1989. Subsection I. Order *Chroococcales* Wettstein 1924, Emend. Rippka et al., 1979, p. 1728–1738. *In* J. T. Staley (ed.), Bergey's manual of systematic bacteriology, vol. 3. Williams and Wilkins, Baltimore.
40. **Waterbury, J. B., S. W. Watson, F. W. Valois, and S. G. Franks.** 1986. Biological and ecological characterization of the marine unicellular cyanobacteria *Synechococcus*. Can. Bull. Fish. Aquat. Sci. **214:**71–120.
41. **Weisse, T.** 1993. Dynamics of autotrophic picoplankton in marine and freshwater ecosystems. Adv. Microb. Ecol. **13:**327–370.
42. **Whitton, B. A., N. G. Carr, and I. W. Craig.** 1971. A comparison of the fine structure and nucleic acid biochemistry of chloroplasts and blue-green algae. Protoplasma **72:**325–357.
43. **Wood, A. M., and D. Townsend.** 1990. DNA polymorphism within the WH7803 serogroup of marine *Synechococcus* spp. (cyanobacteria). J. Phycol. **26:**576–585.
44. **Zyskind, J. W., and D. W. Smith.** 1992. DNA replication, the bacterial cell cycle, and cell growth. Cell **69:**5–8.